AIAA 80-1001R

Interior Noise Control by Fuselage Design for High-Speed Propeller-Driven Aircraft

J. D. Revell* and F. J. Balena†
Lockheed-California Company, Burbank, Calif.
and
L. R. Koval‡
University of Missouri, Rolla, Mo.

An analytic study was performed to define the acoustical treatment weight penalties that are required to provide an interior noise level of 80 dBA in propfan-powered aircraft at Mach 0.8 cruise. The prediction method, described in a companion paper, combines Koval's theory for cylindrical shell noise transmission loss (TL) with Beranek and Work's method for multilayered acoustic treatment analyses. Three fuselage diameters are studied which represent commuter, narrow-body, and wide-body aircraft. The calculated acoustic treatment weight penalties range from 1.7 to 2.4% of aircraft takeoff gross weight (TOGW) for add-on designs. Advanced noise reduction designs, those which permit structural modifications, reduce the acoustic treatment weight penalties to 1.5% TOGW for aluminum aircraft and from 0.74 to 1.4% TOGW for composite fuselage construction. The wide-body results agree with the weight penalty estimates of an earlier turboprop aircraft study.

Introduction

RAPIDLY escalating fuel costs have generated renewed interest in turboprop aircraft owing to their high propulsive efficiency. Propeller-driven aircraft have historically exhibited high interior noise levels at the blade passage frequency and its harmonics. This has generated concern about the acceptability of future propeller aircraft and the weight penalties required for interior noise control. The analytic study results presented in this paper were taken from a NASA Langley funded study of interior noise control for propfan-powered aircraft.[1] A description of the analytic method used for interior noise predictions is presented in a companion paper.[2] An interior noise goal of 80 dBA was selected, since this level was considered competitive with the quietest turbofan aircraft in service at this time. The acoustical treatment mass penalties required to achieve this goal were calculated for three propfan-powered aircraft designed for Mach 0.8 cruise at an altitude of 30,000 ft. The configuration TL was calculated via a synthesis of Koval's theory for cylindrical shell noise transmission loss[3] with Beranek and Work methods[4-6] for add-on noise-control element performance. Two design philosophies were used to achieve the 80-dBA interior noise goals for each of the three aircraft studied: 1) an "add-on" design which did not modify the strength or stiffness of the existing sidewall structure and would be appropriate for existing aircraft; 2) an "advanced" design which did allow modifications of the sidewall structure.

The add-on approach permits the use of conventional aircraft structures with added damping material on the outer wall and heavy interior trim panels. Advanced designs are much stiffer than conventional aircraft structures and they are also combined with heavier than normal trim panels to achieve the desired interior noise goal. Both design philosophies advantageously employed the "double-wall effect," and produced configurations in which the total surface density of the fuselage wall was divided nearly equally between the outer wall and the trim; however, the advanced designs always weighed less. The weight penalty calculated for the add-on wide-body design was essentially identical to that determined in Ref. 7 for the same aircraft. A simple double-wall mass law analysis was used in the earlier study and confirmation of that earlier weight penalty estimate is considered significant.

Aircraft Configuration

Three aircraft were defined at a preliminary design level of refinement for this study—a wide-body, a narrow-body, and a small business aircraft, shown in Figs. 1, 2, and 3, respectively. Design and mission characteristics are summarized for these aircraft in Table 1. The wide-body aircraft selected for this study is a 200-passenger, 2778-km (1500-n.mi.) design that was developed during a reduced energy consumption aircraft technology (RECAT) study. This aircraft has four wing-mounted turboshaft engines and an eight-bladed Hamilton Standard designed propfan. During the RECAT study of Ref. 7, the wide-body design was optimized for minimum fuel usage for its intended mission. Both the narrow-body and the business size aircraft designs are a result of previous Lockheed preliminary design studies of turbofan-powered aircraft applicable to the short-haul

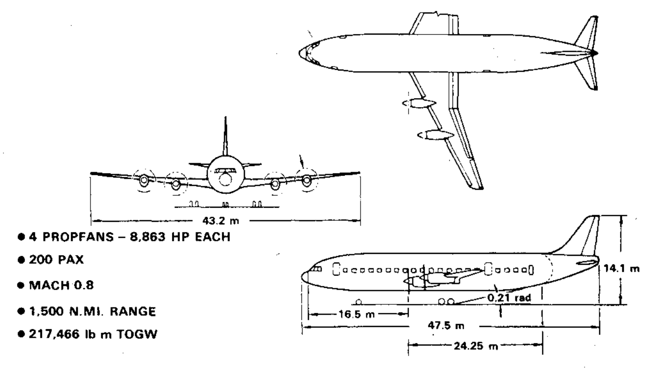

Fig. 1 General arrangement—wide body.

Presented as Paper 80-1001 at the AIAA 6th Aeroacoustics Conference, Hartford, Conn., June 4-6, 1980; submitted July 23, 1980; revision received June 16, 1981.

*Research and Development Scientist, Acoustics Department. Associate Fellow AIAA.

†Research and Development Engineer, Acoustics Department.

‡Professor, Department of Mechanical and Aerospace Engineering. Member AIAA.

market. They have been reconfigured to incorporate propfan propulsion and sized for minimum fuel usage. The baseline gross weights given in Table 1 include the weight of a thermal/acoustic fiberglass blanket and decorative interior trim panel.

Prediction Method

The analytical method used to predict interior noise is described in some detail in Ref. 2 and will be summarized only briefly in this paper. Interior noise is determined from predicted fuselage sound transmission loss (STL) and predicted (or measured) exterior noise by the following procedure (refer to Fig. 4):

1) Calculate the STL of a small flat skin panel bounded by stiffeners.

2) Calculate the STL of an untreated stiffened cylinder.

3) Calculate the STL of a small flat skin panel with added acoustic treatments.

4) The STL of the stiffened but untreated cylinder is then defined as the lower envelope of 1 and 2 above.

5) The STL increment due to the acoustic treatment is obtained by subtracting 1 from 3 above.

6) Treated cylinder STL is then obtained by adding 4 and 5 above.

7) Treated cylinder noise reduction is determined by assuming that the cabin interior is semireverberant and that the interior absorption is uniformly distributed over all the interior surfaces.

8) Predicted interior noise is then obtained by subtracting the configuration noise reduction from the exterior noise.

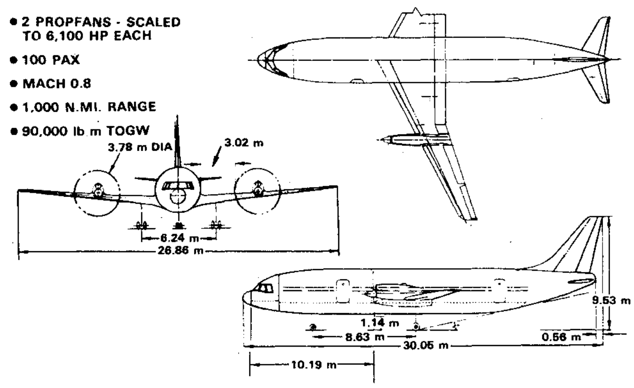

Fig. 2 General arrangement—narrow body.

Study Assumptions

Interior noise calculations were performed using Koval's[3] theory for cylindrical shell STL. In this approach the amplitude and graze angle of the incident sound is assumed constant over the entire length of the structure. The cir-

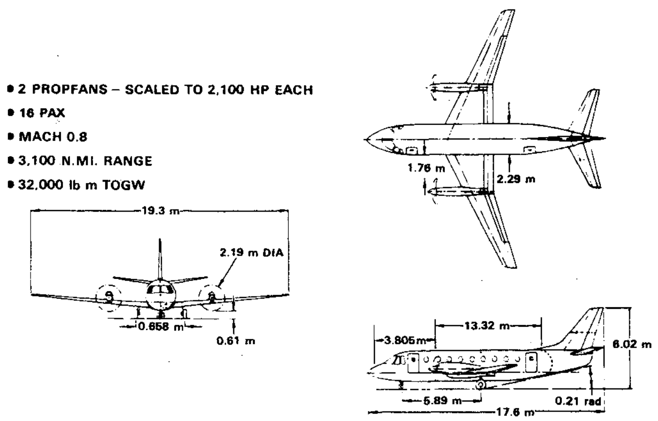

Fig. 3 General arrangement—business aircraft.

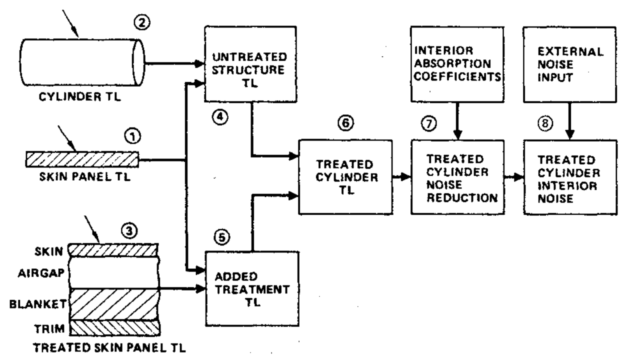

Fig. 4 Method used to calculate treated cylinder noise reduction.

Table 1 Aircraft design and mission characteristics

	Wide body	Narrow body	Business aircraft
Range, km (n.mi.)	2778 (1500)	1852 (1000)	5741 (3100)
No. pax	200	100	16
Cruise speed, Mach number	0.8	0.8	0.8
Initial cruise altitude, m (ft)	9144 (30,000)	9144 (30,000)	9144 (30,100)
Field length, m (ft)	2134 (7000)	1524 (5000)	1524 (5000)
Fuselage diameter, m (ft)	6.12 (19.8)	3.91 (12.8)	2.24 (7.3)
Fuselage length, m (ft)	47.5 (155.8)	30.0 (98.58)	17.6 (57.67)
Seat pitch, m (ft)	0.864(2.8)	0.864(2.8)	0.864(3.2)
Seating arrangement	8-abreast	6-abreast	2-abreast
TOGW, kgm (lbm)	98,641 (217,466)	40,823 (90,000)	14,515 (32,000)
Propulsion	STS 476	STS 476	STS 476
Propfan diameter, m (ft)	3.84 (12.6)	3.78 (12.4)	2.19 (7.2)
Number of blades, m/s (ft/s)	244 (800)	244 (800)	244 (800)
Tip speed	8	8	8
Power loading, kW/m^2 (hp/ft^2)	293 (37.1)	242 (30.6)	244 (28.3)
No. engines,	4	2	2
Cruise thrust, N/engine (lb/engine)	14,813 (3330)	13,345 (3000)	4182 (940)
Blade passage frequency, Hz	162	164	283
Propeller efficiency	0.837	0.852	0.854
Sea-level static thrust/ takeoff gross weight	0.26	0.27	0.27
Maximum power at SLS, kW (hp)/engine	6609 (8863)	4459 (6100)	1566 (2100)
Sea-level static thrust, N/engine (lb/engine)	62,876 (14,135)	55,247 (12,420)	19,216 (4320)

cumferential distribution of incident sound is assumed to be a Fourier-Bessel expansion of an incident plane wave as described by Koval[3] following the earlier work of Smith.[9] However, the estimated axial directivity for two-engine and four-engine aircraft derived from Hamilton Standard data[8] and shown in Figs. 5 and 6 exhibit variable amplitude and graze angle with axial position. Consequently, the fuselage was divided into seven segments and calculations were performed for each segment as though it represented the entire fuselage (see Table 2). Each segment spanned a range of incidence angles and the average STL of the segment was obtained by an antilogarithmic summation and average of the STL calculated at several specific angles of incidence within that segment. For the peak noise region of segment 4, the range of incidence angles is quite large and fifteen equally spaced angles of incidence are used to obtain the segment STL. Weight penalties to achieve a specified interior noise level are defined by the increments of the treated surface density above the baseline values in Table 3.

The segment sound pressure levels shown in Figs. 5 and 6 were considered overly conservative and would result in excessive weight penalties. Therefore the segment weight penalties determined from the assumed segment sound pressure levels of Figs. 5 and 6 were reduced by continuously varying the weight penalty over the length of the segment. The local weight penalty was determined from the local exterior noise level rather than the nominal segment sound pressure level used for the segment STL calculation. At a given axial position, a uniform weight penalty was assumed to be required over 60% of the fuselage circumference—the fraction above the floor. The narrow-body and business aircraft have two engines, and a normalized propeller tip clearance of 0.8 propeller diameters was used for both aircraft. For the four-engine wide-body aircraft the inboard and outboard propeller tip clearances were 1.2 and 2.3 propeller diameters, respectively.

Figure 7 describes the three harmonic distributions of the estimated exterior overall sound pressure levels (OASPL) that

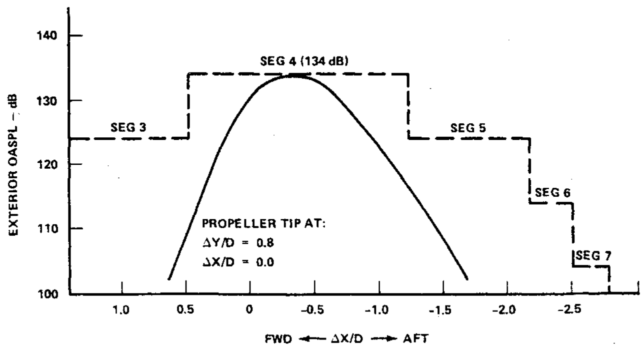

Fig. 5 Two-engine narrow-body aircraft exterior noise signature and treatment segments.

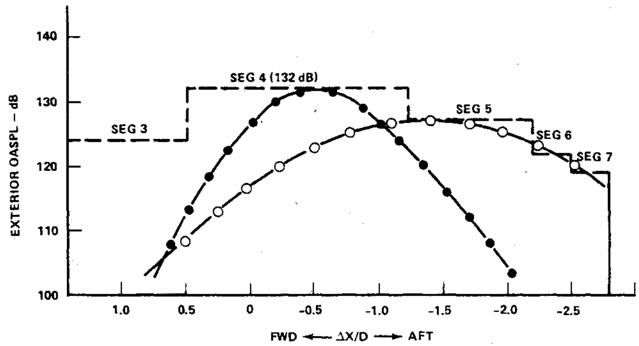

Fig. 6 Four-engine narrow-body aircraft exterior noise signature and treatment segments.

Table 2 Fuselage segment properties

Propeller tip clearance $(\Delta y/D)_{IB}$	$(\Delta y/D)_{OB}$	Segment no.	Position $(X-X_{IB})/D$	Location[a]	ΔOASPL for segment,[b] dB	Local graze angle of incident sound wave from: Inboard prop rad	Inboard prop deg	Outboard prop rad	Outboard prop deg
A. Two-engine aircraft									
0.8	N.A.	3	1.42	Forward edge Seg. 3	−10	2.63	151	N.A.	
			0.47	Aft edge Seg. 3		2.10	120	N.A.	
		4	0.47	Forward edge Seg. 4	0	2.10	120	N.A.	
			0	Inboard engine propeller disk plane		1.57	90	N.A.	
			−1.23	Aft edge Seg. 4		0.58	33	N.A.	
		5	−1.23	Forward edge Seg. 5	−10	0.58	33	N.A.	
			−2.18	Aft edge Seg. 5		0.35	20.0	N.A.	
		6	−2.18	Forward edge Seg. 6	−20	0.35	20.2	N.A.	
			−2.48	Aft edge Seg. 6		0.31	17.8	N.A.	
		7	−2.48	Forward edge Seg. 7	−30	0.31	17.8	N.A.	
			−2.78	Aft edge Seg. 7		0.28	16.1	N.A.	
B. Four-engine aircraft									
		3	1.42	Forward edge Seg. 3	−10	2.44	140	2.12	127
			0.47	Aft edge Seg. 3					
		4	0.47	Forward edge Seg. 4	−2	1.94	111	1.77	102
			−0.27	Inboard disk plane		1.39	77	1.45	83
			−1.0123	Outboard disk plane		0.87	49.9	1.16	66.2
			−1.23	Aft edge Seg. 4		0.77	44.3	1.08	61.9
		5	−1.23	Forward edge Seg. 5	−7	0.77	44.3	1.08	61.9
			−2.18	Aft edge Seg. 5		0.50	28.8	1.08	46.5
		6	−2.18	Forward edge Seg. 6	−12	0.50	28.8	0.81	46.5
			−2.48	Aft edge Seg. 6		0.45	25.8	0.75	42.8
		7	−2.48	Forward edge Seg. 7	−15	0.45	25.8	0.75	42.8
			−2.78	Aft edge Seg. 7		0.41	23.3	0.69	39.6

[a] Segments 1 and 2 forward of those described in this table are found not to require more than the baseline acoustic treatment and therefore are omitted. [b] ΔASPL = (OASPL) − (134 dB).

Table 3 Baseline surface density data

Component	Wide body kg/m^2	Wide body psf	Narrow body kg/m^2	Narrow body psf	Business aircraft kg/m^2	Business aircraft psf
A. Aluminum aircraft						
Outer wall	9.18	1.88	6.25	1.28	4.69	0.96
Fiberglass blanket	0.73	0.15	0.73	0.15	0.49	0.10
Baseline trim panel	1.61	0.33	1.61	0.33	1.61	0.33
Total wall	11.52	2.36	8.59	1.76	6.79	1.39
B. Composite structure						
Outer wall	6.40	1.31	4.35	0.89	3.27	0.67
Fiberglass blanket	0.73	0.15	0.73	0.15	0.49	0.10
Baseline trim panel	1.61	0.33	1.61	0.33	1.61	0.33
Total wall	8.74	1.79	6.69	1.37	5.37	1.10

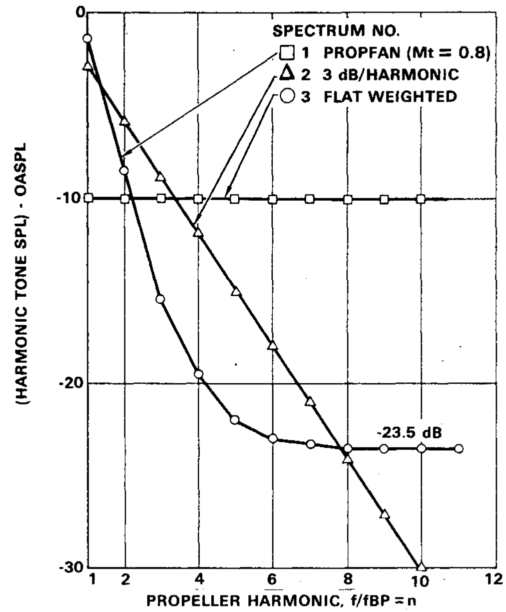

Fig. 7 Relative tone SPL vs harmonic number.

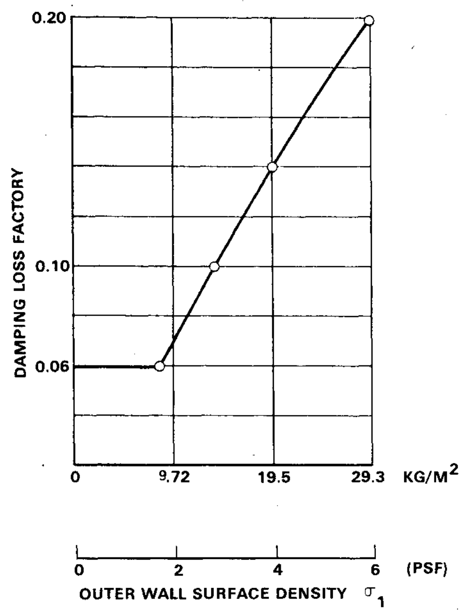

Fig. 8 Damping loss factor vs outer-wall surface density.

were used to calculate interior noise. Spectrum number 1 is derived from the Hamilton Standard data of Ref. 8 and is considered the most realistic of the three distributions. Spectrum numbers 1 and 2 usually required the same weight penalties to achieve an 80-dBA interior noise level. When spectrum number 3 was used the resulting interior noise was about 5 dBA lower than that calculated for the other harmonic distributions. The results reported in this paper were obtained using the harmonic distributions of spectrum 1.

A damping loss factor of 6% was assumed for the baseline aircraft structure. A schedule of damping loss factor (attainable by the addition of viscoelastic materials) vs outer wall weight has been established for each aircraft type for the add-on designs. It was assumed that the added damping treatments did not alter the stiffness properties of the baseline structure. The damping schedule used for the wide-body, and shown in Fig. 8, is based on unpublished Lockheed studies and the methods of Refs. 10 and 11.

In order to investigate the benefits to be obtained by increases of outer wall stiffness, a realistic schedule of the weight or mass increase associated with increased stiffness was required. A preliminary design study determined the section properties required to increase the stiffness of the baseline structures by prescribed amounts. These data were used to establish stiffness and mass relationships for all three aircraft for both aluminum and graphite/epoxy structures, as shown in Figs. 9 and 10. The advanced designs allowed stiffness increases and outer wall mass was increased accordingly. For these designs the damping loss factor was held constant for all stiffness levels.

Noise Reduction Results

Baseline Noise Reduction Results

The Koval theory was used to predict STL for the baseline wide-body aluminum fuselage as a function of angle of incidence (see Fig. 11). Similar predictions were made for each of the three aircraft types for both aluminum and graphite/epoxy structures but they are not shown here. The wide-body STL results are nearly identical with those for the narrow-body and business aircraft when the frequency scale is normalized by the ring frequency. At shallow graze angles, transmission loss increases with frequency and is interrupted by a characteristic STL decrease in the vicinity of the ring frequency. Near normal incidence the ring frequency effect is not evident. As shown in Fig. 11, the blade passage frequency and its first two harmonics fall within the ring frequency trough in transmission loss. Noise reduction and weight of the baseline aluminum and composite structures provide a reference point for comparison with the add-on and advanced design performance.

Results for Add-On Designs

Although weight penalties were calculated for all segments, only the results for segment 4 are shown in Fig. 12. Segment 4

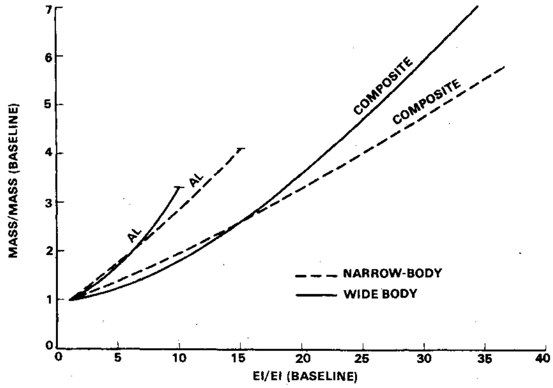

Fig. 9 Outer wall mass vs stiffness level for wide-body and narrow-body aircraft.

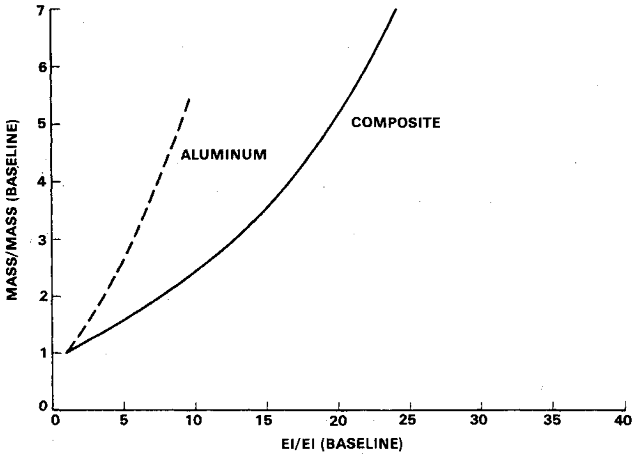

Fig. 10 Outer wall mass vs stiffness level for business aircraft.

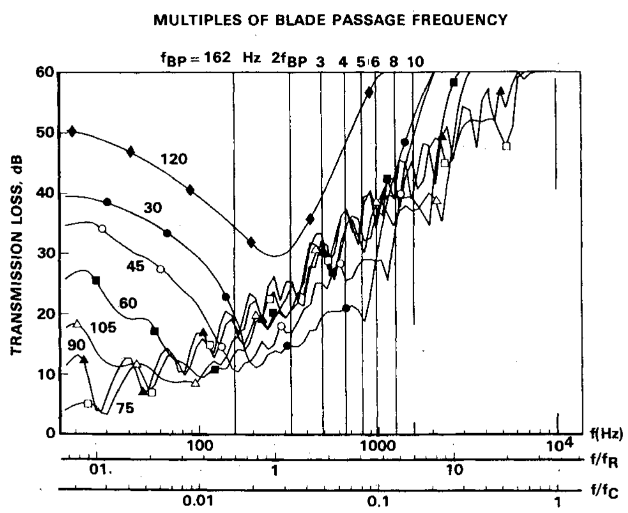

Fig. 11 STL characteristics of wide-body aluminum aircraft outer wall structure.

is the largest segment and includes the propeller plane of rotation. The total weight penalty was obtained by summing the contribution for all segments. Each curve in Fig. 12 represents the noise-control performance of an add-on configuration with loss factor η and outer wall surface density σ_l. For a given outer wall weight the trim panel weight was varied to obtain 80 dBA. Total surface density is plotted as a function of the absolute interior noise and the change in exterior noise level. Thus, if the exterior noise level changes by a specified amount the new total surface density can be

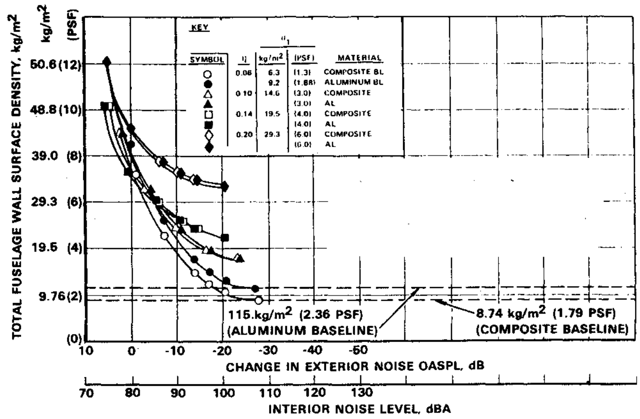

Fig. 12 Four-engine wide-body interior noise.

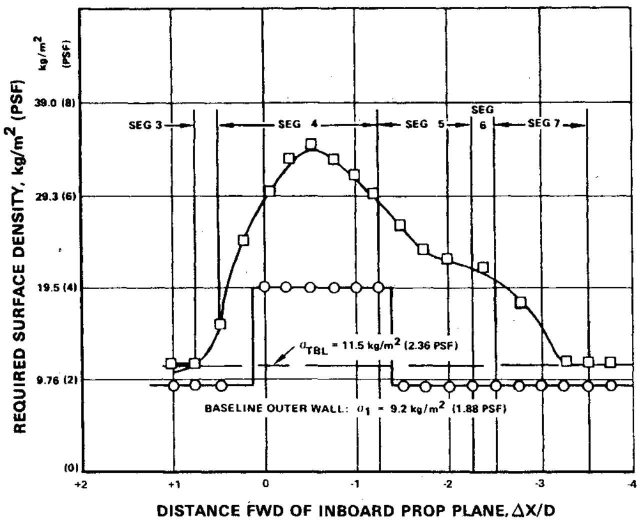

Fig. 13 Four-engine wide-body surface density distribution—add-on design.

determined. An interior noise level of 80 dBA is achieved with a total surface density of over 7 psf including a 4-psf trim panel—a nearly equal division of weight between the outer wall and interior trim, as would be expected from double-wall mass law theory.

The axial distribution of the wall surface density required to achieve an 80-dBA interior level for the wide-body aircraft is shown in Fig. 13. Segment 4 was the only segment which required a heavier than baseline outer wall. The effect of the outboard engine is evident in Fig. 13, requiring heavier trim panels in segments 5-7. Summaries of the acoustic treatment mass penalties for the aluminum and composite aircraft add-on designs are presented in Table 4. Composite aircraft designed for the same mission requirements as their aluminum counterparts would have been considerably lighter in weight and have resized power plants. Lower thrust requirements would translate into smaller sized propfans with smaller acoustic treatment areas and lower mass penalties. However, complete redesigns of the composite aircraft are beyond the scope of this study and the composite aircraft were assumed to have the same TOGW as their aluminum counterparts. This assumption reduced the percentage of TOGW required to achieve 80 dBA in the composite aircraft. On the other hand, resized composite aircraft with a smaller treatment area requirement would have required lower absolute mass additions to achieve 80 dBA and would have had lower TOGW's.

The acoustical treatment mass penalty requirements for the aluminum wide-body are consistent with the RECAT study[7] results. However, the current study results represent a higher

Table 4 Add-on acoustic treatment mass penalties

Aircraft No. engines	Takeoff gross weight, kg (lb)	Fuselage diameter, m (ft)	Propeller diameter, m (ft)	Baseline outer wall surface density, kg^2 (psf)	Blade passage frequency, Hz	Mass penalty, kg (lb)	TOGW, %
A. Aluminum aircraft							
WB/4	98,641 (217,466)	6.10 (20.00)	3.84 (12.6)	9.17 (1.88)	162	2283 (5033)	2.31
NB/2	40,823 (90,000)	3.90 (12.80)	3.78 (12.4)	6.25 (1.28)	164	742 (1635)	1.82
SBA/2	14,515 (32,000)	2.23 (7.33)	2.19 (7.2)	4.68 (0.96)	283	250 (551)	1.72
B. Composite aircraft							
WB/4	98,641 (217,466)	6.10 (20.00)	3.84 (12.6)	6.39 (1.31)	162	2441 (5381)	2.47
NB/2	40,823 (90,000)	3.90 (12.80)	3.78 (12.4)	4.34 (0.89)	164	860 (1895)	2.11
SBA/2	14,515 (32,000)	2.23 (7.33)	2.19 (7.2)	3.27 (0.67)	283	266 (586)	1.83

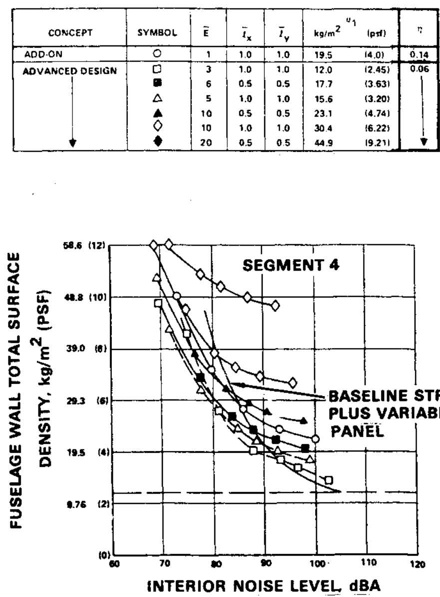

Fig. 14 Wide-body aluminum advanced vs add-on noise control.

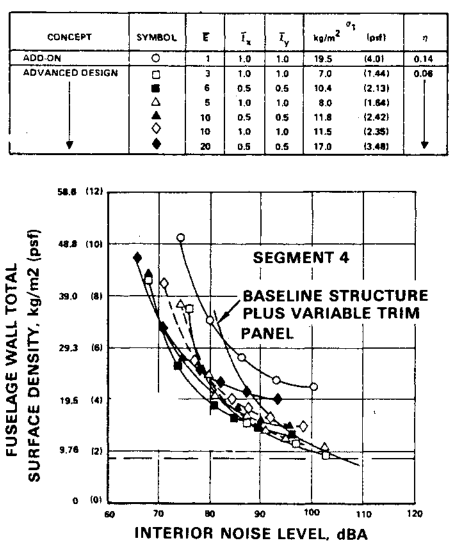

Fig. 15 Wide-body composite advanced vs add-on noise control.

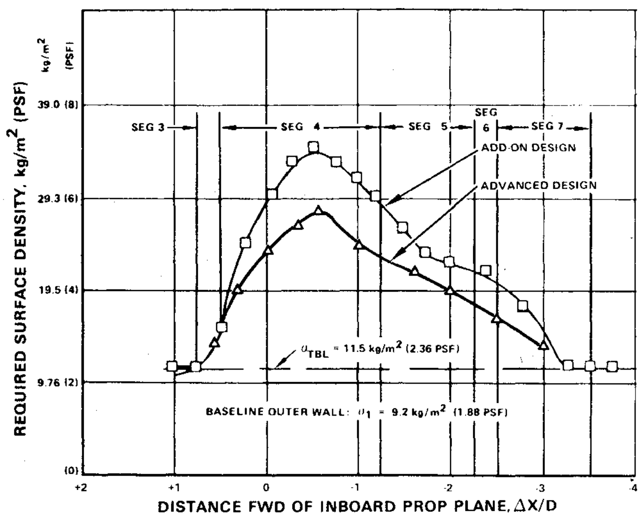

Fig. 16 Four-engine wide-body surface density distributions—aluminum.

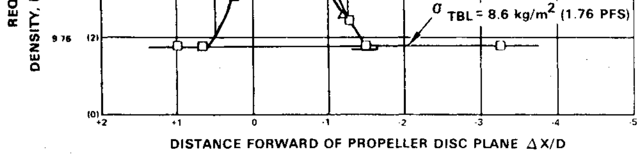

Fig. 17 Two-engine narrow-body surface density distributions—aluminum.

surface density penalty applied to a somewhat smaller treatment area. The agreement with Ref. 7 implies that the estimated 17% net savings in fuel consumption for propfan-powered aircraft relative to comparable turbofan-powered aircraft are still valid.

Results for Advanced Designs

The schedules of fuselage outer wall mass required to achieve increased stiffness which are shown in Figs. 9 and 10 were utilized for the advanced noise reduction design studies. Variation of the outer wall stiffness was the key difference between the add-on and advanced noise reduction designs. The ultimate objective of both design philosophies was a minimum acoustic treatment weight for an 80-dBA interior noise level.

Figures 14 and 15 summarize the results of the advanced design study for wide-body aluminum and composite aircraft,

Table 5 Summary of mass penalty data

Aircraft type:	Wide body			Narrow body			Business		
TOGW:	98,641 kg (217,466 lb)			40,823 kg (90,000 lb)			14,515 kg (32,000 lb)		
Concept	kg	lb	TOGW, %	kg	lb	TOGW, %	kg	lb	TOGW, %
Add-on aluminum	2283	5033	2.31	742	1635	1.82	250	551	1.72
Advanced aluminum	1523	3358	1.54	616	1357	1.51	225	445	1.55
Add-on composites	2441	5381	2.47	860	1895	2.11	266	586	1.83
Advanced composites	1009	2225	1.02	573	1264	1.40	107	237	0.740

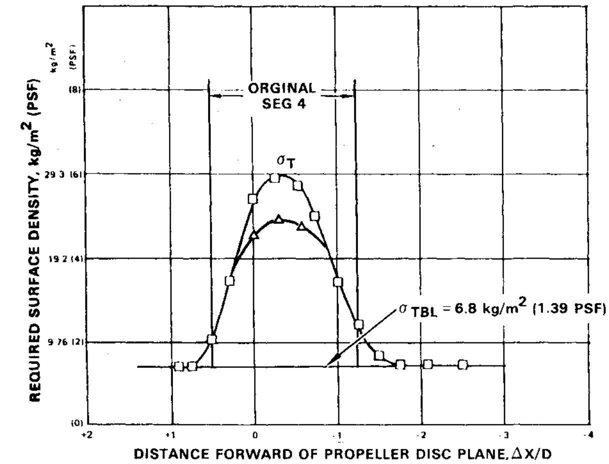

Fig. 18 Business aircraft surface density distributions— aluminum.

respectively. For these analyses, the outer wall with surface density σ_t and relative stiffness level $\bar{E}$ were combined with a variable weight trim panel. Each plot contains the baseline zero penalty surface density for the outer wall and for the combined baseline outer wall plus trim panel weight. The advanced aluminum configuration surface density was more than 2 psf lower than the add-on for the aluminum wide-body and nearly 4 psf lower for the composite for an 80-dBA interior. It should be noted that the data in Figs. 14 and 15 pertain to segment 4, and spectrum number 1 for the wide-body aircraft. Similar results were calculated for the narrow-body and small business aircraft but are not included here.

The minimum surface densities required for 80 dBA for each segment for all three aluminum aircraft were then used to obtain the surface density distributions shown in Figs. 16-18. A comparison between the surface density distributions for the add-on and advanced designs is also shown. Similar data were obtained for the composite aircraft designs but are not included herein. These results show improved performance (reduced weight) for the advanced designs. Surface density weight penalties are incurred in segment 4 for the two-engine aircraft while the four-engine wide-body requires surface density increases in segments 4-7.

Table 5 summarizes the integrated acoustic treatment weight penalties for both the add-on and the advanced noise reduction designs. As mentioned above, the advanced designs show significant weight penalty reductions relative to the add-on designs. It should also be noted that for the advanced designs, the composite aircraft weight penalties are lower than those for the aluminum aircraft whereas the add-on design penalties are nearly identical. These data show that increases in outer wall stiffness are beneficial when combined with increases in wall and trim panel weight. The benefits of composite structures are not realized in the add-on configurations, since they rely on increases in outer wall and trim panel surface density for interior noise control. It is conjectured that stiffening the outer wall increases the frequencies at which the outer wall is highly transmissive, and that the double-wall treatment is more efficient at these higher frequencies.

Concluding Remarks

Sidewall noise-control weight penalties have been estimated for propfan-powered aircraft with an interior noise level of 80 dBA. This noise level is competitive with the quietest current technology turbofan aircraft and is considered acceptable. The weight penalties for add-on designs range from 1.7 to 2.5% of aircraft TOGW. Advanced noise reduction designs were also identified in this study and they reduced the noise-control weight penalties to 1.5% TOGW for the aluminum aircraft and from 0.7 to 1.4% for aircraft constructed with composite materials. The method of analysis is considered conservative in some respects, as discussed in Ref. 2.

The weight penalties estimated herein are large by comparison with that required for current technology turbofan aircraft. However, the noise-control weight penalties are only one element in a more complex cost/benefit system analysis that needs to be performed.

References

[1] Revell, J.D., Balena, F.J., and Koval, L.R., "Analytical Study of Interior Noise Control by Fuselage Design Techniques on High-Speed, Propeller-Driven Aircraft," NASA CR-159222, April 1980.

[2] Revell, J.D., Balena, F.J., and Koval, L.R., "Analysis of Interior Noise-Control Treatments for High-Speed Propeller-Driver Aircraft," *Journal of Aircraft*, Vol. 19, Jan. 1982, pp. 31-38.

[3] Koval, L.R., "On Sound Transmission Into a Thin Cylindrical Shell Under Flight Conditions," *Journal of Sound and Vibration*, Vol. 48, No. 2, 1976, pp. 265-275.

[4] Beranek, L.L. and Work, G.A., "Sound Transmission Through Multiple Structures Containing Flexible Blankets," *Journal of the Acoustical Society of America*, Vol. 21, No. 4, July 1949, pp. 419-428.

[5] Beranek, L.L., "Acoustical Impedance of Porous Materials," *Journal of the Acoustical Society of America*, Vol. 13, No. 3, Jan. 1942, pp. 248-260.

[6] Beranek, L.L., "Acoustical Properties of Homogeneous Isotropic Rigid Tiles and Flexible Blankets," *Journal of the Acoustical Society of America*, Vol. 19, No. 4, July 1947, pp. 556-568.

[7] Revell, J.D. and Tullis, R.H., "Fuel Conservation Merits of Advanced Turboprop Transport Aircraft," NASA CR-152096, Aug. 1977.

[8] "Propfan and Gearbox Near Field Noise Predictions," Hamilton Standard Division United Technologies, SP15A77, Oct. 1977.

[9] Smith, P.W., "Sound Transmission Through Thin Cylindrical Shells," *Journal of the Acoustical Society of America*, Vol. 29, No. 6, June 1957, pp. 721-729.

[10] Ungar, E., "Damping of Panels," *Noise and Vibration Control*, edited by L. Beranek, McGraw Hill, New York, 1971, Chap. 14, pp. 434-474.

[11] Torvik, P.J. and Strickland, D.Z., "Damping Additions for Plates Using Constrained Viscoelastic Layers," *Journal of the Acoustical Society of America*, Vol. 51, No. 3 (Part 2), 1972, pp. 985-991.